A Journal of the Gesellschaft Deutscher Chemiker

Angewandte International Edition Chemie

GDCh

www.angewandte.org

Accepted Article

Title: Fast Exfoliation and Functionalisation of 2D Crystalline Carbon Nitride by Framework Charging

Authors: Jingjing Jia, Edward R. White, Adam J. Clancy, Noelia Rubio Carrero, Theo Suter, Thomas S. Miller, Paul M. McMillan, Veronika Brázdová, Furio Corà, Chris A. Howard, Cecilia Mattevi, and Milo Shaffer

To be cited as: *Angew. Chem. Int. Ed.* 10.1002/anie.201800875
Angew. Chem. 10.1002/ange.201800875

Link to VoR: http://dx.doi.org/10.1002/anie.201800875
http://dx.doi.org/10.1002/ange.201800875

WILEY-VCH

10.1002/anie.201800875

WILEY-VCH

Fast Exfoliation and Functionalisation of 2D Crystalline Carbon Nitride by Framework Charging

Jingjing Jia, Edward R. White, Adam J. Clancy, Noelia Rubio, Theo Suter, Thomas S. Miller, Kit McColl, Paul F. McMillan, Veronika Brázdová, Furio Corà, Chris A. Howard, Robert V. Law, Cecilia Mattevi,* and Milo S. P. Shaffer*

Abstract: 2D layered graphitic carbon nitride nanosheets offer tunable electronic and chemical properties. However, exfoliation and functionalisation of gCN for specific applications remains challenging. We report a scalable one-pot reductive method to produce solutions of single and few layer 2D gCN nanosheets with excellent stability in a high mass yield (35%) from polytriazine imide. High resolution imaging confirms the intact crystalline structure and identifies an AB stacking. The first successful deliberate organic functionalisation of dissolved gCN is illustrated, providing a general route to adjust their properties.

Graphitic carbon nitride (gCN) has triggered tremendous interest due to its 2D structure, analogous to graphene, but with complementary characteristics.[1] In particular, it offers inherent semiconductivity with tunable band gap and optical absorption,[2] whilst the different chemical valences of N and C create empty sites within the layers.[3] Monolayer/few layer carbon nitride nanosheets (FL-CNs) have been isolated as a new family of 2D layered materials, motivated by their unique photocatalytic activity.[4] Several methods have been adopted to synthesize FL-CNs of various thicknesses/sizes.[5] Unfortunately, many of these processes damage the structure, altering the properties of interest; they are also time-consuming and provide low yields and dilute suspensions, and most work has focused on the disordered heptazine-based gCNs. Polytriazine imide (PTI) has been previously synthesized and characterized using a number of bottom-up approaches.[6] PTI is more crystalline than its heptazine-based counterpart, containing genuine planar layers of imide-bridged triazine units,[7] and its exfoliation into high quality 2D FL-CN crystals is, therefore, attractive. Achieving a non-damaging preparation of 2D few-layered PTI (FL-PTI) in a high yield is still in its infancy, although slow dissolution has recently been reported.[8] Moreover, while covalent functionalisation is a vital tool in tailoring the properties of nanomaterials,[9] to date there has been little direct covalent functionalisation of PTI.

This paper demonstrates a simple, one-pot exfoliation, dissolution, and optional functionalisation of FL-PTI *via* reduction. Reductive charging has been used previously to dissolve a variety of 2D nanomaterials,[10] *via* metal-ammonia solutions and organic charge transfer agents (CTA). The use of sodium naphthalide (NaNp) dissolved in N,N-dimethylacetamide (DMAc) was recently found to be especially effective for the dissolution and functionalisation of single wall nanotubes in a single step.[14] Here the methodology is adapted to gCNs, specifically PTIs.

Successful exfoliation of PTI was achieved by framework charging process (Fig. 1). Sodium is used as the electron source to form naphthalide ions, which act as a CTA. DMAc is an excellent room temperature solvent for naphthalene/ide and anionic nanocarbons, and can be expected to be a good solvent for FL-PTI.[11] NaNp/DMAc solution has a characteristic green color which simplifies reaction monitoring. NaNp/DMAc solutions were added into dried PTI powders at controlled stoichiometry. The reduction and exfoliation process was observed by the color change from the initial brown PTI suspension to dark green after addition of NaNp/DMAc, before finally forming a brilliant orange dispersion of FL-PTI (FL-PTI^{n-}) within minutes (Fig. S1). After removing the remaining insoluble PTI fragments by centrifugation (5000 *g*, 30 min, Fig. S2), a homogeneous golden FL-PTI^{n-} solution with a concentration up to 1.2 mg·mL^{-1} was obtained (Fig. S1c), which was stable under N_2 for >1 year (Fig. S3a). Deposited FL-PTI^{n-} nanosheets display hexagonal geometry with a height of 1-2 nm (Fig. S3), indicating that they comprise only a few PTI layers, based on a 3.52 Å layer thickness.[6b] The negative charges from the naphthalide are likely to be rapidly transferred to the PTI, due to the high reduction potential of naphthalide (*ca.* 3.0 eV vs SHE);[12] accelerated by the small size of the PTI platelets and the intrinsic pores.[13] The partially dissociated Na^+ counterions leave a net unscreened negative charge on the PTI^{n-} (Fig. S4a), leading to short range Coulombic repulsions and hence exfoliation of PTI into solvated FL-PTI^{n-} sheets (Fig. 1), analogous to reduced nanocarbons[10a, 14] and transition metal dichalcogenides.[10b] Upon air exposure, the FL-PTI reagglomerate slowly (~2 months, Fig. S5b); the reduced rate compared to charged SWCNTs,[14b] likely relates to the lower aspect ratio and localisation/low mobility of the charges on the framework.[15]

[*] J. Jia, E. R. White, A. J. Clancy, N. Rubio, M. S. P. Shaffer,
Dept. Chemistry, Imperial College London,
London, SW7 2AZ, UK.
E-mail: m.shaffer@imperial.ac.uk
C. Mattevi
Dept. Materials, Imperial College London,
London, SW7 2AZ, UK
E-mail: c.mattevi@imperial.ac.uk
T. Suter, T. S. Miller, P. F. McMillan,
K. McColl, V. Brázdová, F. Corà,
Dept. Chemistry, University College London,
London, WC1H 0AJ, UK.
C. A. Howard
Dept. Physics and Astronomy, University College London,
London, WC1E 6BT, UK.

Electronic supplementary information (ESI) for this article is given via a link at the end of the document.

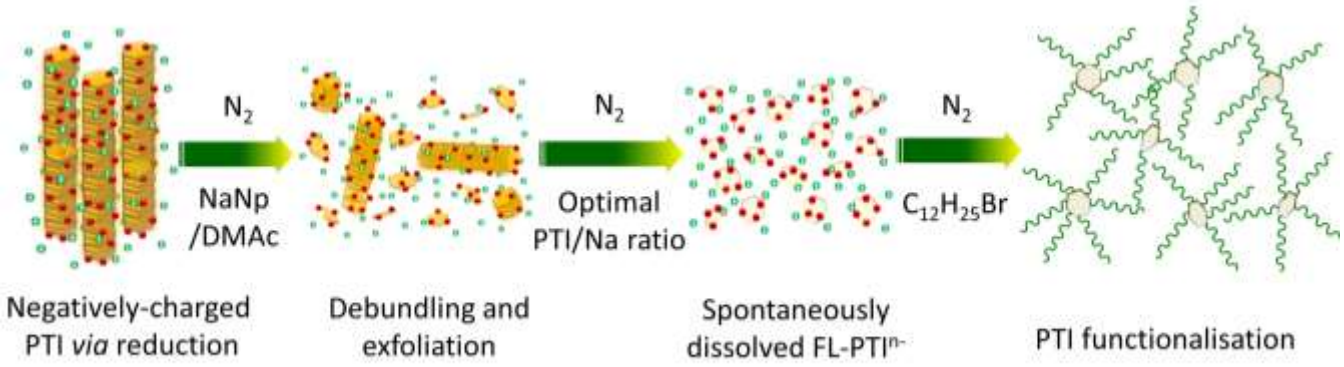

Figure 1. Schematic of charging and exfoliation of PTI.

The charging ratio (molar [PTI framework atoms]:Na (ESI), weighted M_w(PTI) = 13.14) and initial PTI loading (mg PTI/ mL of DMAc) are two vital factors affecting the exfoliation, controlling both the yield (mass fractions of PTI) and concentration of solubilised FL-PTI^{n-}. Increasing the degree of charging (*i.e.* lower PTI:Na), at a static PTI loading initially led to an improved yield of FL-PTI^{n-} (4.1 wt% to 34.5 wt%) due to the enhanced Columbic repulsion (Fig. 2a). However, further increasing charge (PTI:Na < 7) reduced the yield. Similar effects have been observed in charged nanocarbon solutions, attributed to Na^+ condensation and charge screening.[11, 16] The optimum Na concentration for exfoliation of PTI is 15 mM (*i.e.* 7:1 PTI:Na for 1.4 mg·mL^{-1}, Fig. 2a), comparable to ~10 mM identified for the exfoliation of Na-reduced graphite of similar geometry.[16] At the highest charge regimes, the charge on the PTI saturates (at PTI:Na ratio of ~5), as observed by the green tinge of unreacted NaNp (Fig. 2a). On varying the initial PTI loading (Fig. 2b), the concentration of dissolved FL-PTI^{n-} scales linearly, giving a consistent yield between 31–35 wt%, indicating that there may be an intrinsically soluble portion of the starting material. The residue, isolated after centrifugation may contain defects that bind the layers; indeed, qualitatively, the undissolved residue appears disordered by SEM (Fig. S2c). The maximum concentration of FL-PTI^{n-} is ~1.2 mg·mL^{-1} from a PTI loading of 3.5 mg·mL^{-1}. Further increases in PTI loading did not increase the concentration, indicating the solution is saturated (Fig. 2b). Exfoliation increases the surface area of the powders determined by nitrogen adsorption (Fig.S7).

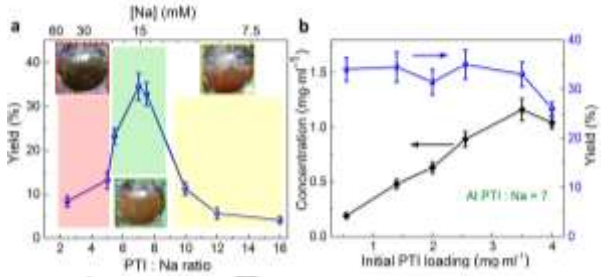

Figure 2. (a) FL-PTI^{n-} yield versus PTI:Na ratio/[Na], 1.4 mg·mL^{-1} PTI. Yellow, green and red rectangles correspond to low, to high [Na] respectively with inset photographs showing resultant FL-PTI^{n-} dispersions. (b) Effect of initial PTI loading on the concentration/yield of FL-PTI^{n-} dissolution (7:1 PTI:Na ratio).

Aqueous FL-PTI dispersions are desirable for environmentally benign processing; however, pristine PTI are poorly soluble in water due to their strong interlayer interactions (6 h probe sonication was found to give a concentration <0.2 mg mL^{-1}). The framework charging process overcomes the strong interlayer interactions and accelerates solubilisation in DMAc, allowing the removal of the intrinsically insoluble fraction of the pristine PTI. The FL-PTIs can then be recovered from the DMAc by solvent exchange and the resultant FL-PTI can be transferred into water by solvent exchange, reaching a saturated concentration of 3.5 mg·mL^{-1}. Atomic force microscopy (AFM) confirms an excellent dispersion of FL-PTI in water (Fig. 3a), with corresponding heights of 0.33-3.2 nm (avg. 1.11 nm, Fig. 3b and S6), suggesting that the nanosheets mostly comprise ~3 PTI layers, although some monolayers are present. Representative energy dispersive X-ray spectroscopy (EDX) maps show uniform dispersion of C and N throughout the whole hexagonal area of the exfoliated FL-PTI nanosheet (Fig 3c-e). High-resolution transmission electron microscopy (HRTEM) micrographs show intact PTI crystallites with regular hexagonal geometry and clear facets (Fig. 4a). Notably, no defect holes or dislocations were observed, confirming the non-destructive nature of the framework charging exfoliation, as well as the high quality of the starting material. Both AFM and STEM (Fig.s 3 & 4, S6, & S8) show flakes with a broad lateral size distribution, up to around 100 nm. The fast Fourier transform (FFT) of the unfiltered HRTEM image shows a hexagonal lattice, demonstrating a single crystal exfoliated FL-PTI (Fig 4a and further examples in S9).[17] The minimum reciprocal lattice vector, G_{min}, is 1.4 nm^{-1}, giving a lattice constant $\boldsymbol{a}$ = (2/√3)G_{min} = 8.5 Å, consistent with the reported values from Br^- intercalated PTI.[15] Two possible stacking models can be considered for the FL-PTI: AB stacking with aligned voids forming c-axis channels, and AC stacking without channels in two adjacent layers (Fig. S10a). Comparing simulated electron diffraction patterns of these two models with the experimental selected area electron diffraction (SAED) data, the AB stacking structure is the better fit for the FL-PTI nanosheets (Fig. 4b-d and S10b), likely stabilised by the Br^- ions detected by EDX (Fig. S11).

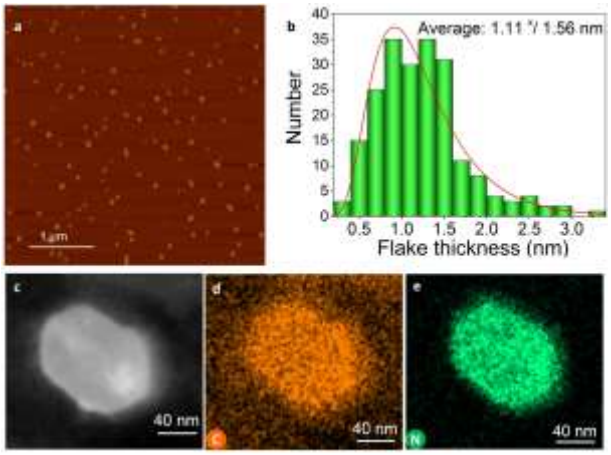

Figure 3. (a) AFM image of FL-PTI nanosheets. (b) PTI thickness histogram (n>200). Mean value is derived from a lognormal distribution. (c) STEM image and EDX elemental maps of C (d) and N (e) on a FL-PTI nanosheet. The background C signal in (d) is due to the carbon TEM support.

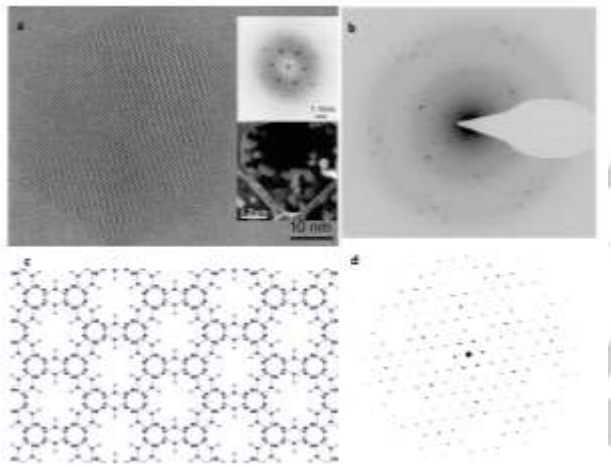

Figure 4. (a) HRTEM image of a FL-PTI nanosheet. Top inset: FFT of the HRTEM image, showing a single crystal hexagonal structure. Bottom inset: STEM image, indicating the layered structure of FL-PTI (b) SAED pattern of a FL-PTI nanosheet. (c) Schematic of the AB stacking in a bilayer. (d) Simulated electron diffraction pattern from the AB crystal structure.

The FL-PTI^{n-} synthesised in DMAc solution provides a versatile platform for covalent functionalisation of PTI, comparable to negatively charged graphene and boron nitride nanotube counterparts.[16, 18] Pristine PTI and FL-PTI nanosheets are thermally stable up to ~700 and 670˚C, respectively (Fig. 5a and Figure S16); the slightly depressed decomposition temperature for FL-PTI reflects its few-layered character. Functionalisation can be performed *via* simple addition of an alkyl halide to the reduced nanomaterial. After functionalisation by reaction with dodecyl bromide, a 10 wt% mass loss can be observed in thermogravimetric analysis/evolved-gas mass spectrometry (TGA-MS), relative to controls; the weight loss correlates with a m/z peak at 57, attributed to $C_4H_9^+$ from the grafted $C_{12}H_{25}$ alkyl chain (Fig. 5a). During the alkylation reaction, the solution changes from a clear golden, to a turbid pale yellow appearance; as the depletion of the negative charges progresses, the Coulombic stabilization is lost, leading to agglomeration and increased light scattering (Fig. 5b, S1c and S12). FTIR (Fig. S20) and solid state NMR were insufficiently sensitive to detect grafting, though deuterated samples (Scheme S1) showed characteristic TGA-MS features (Fig. S18). Nevertheless, X-ray photoelectron spectroscopy (XPS) measurements confirmed the covalent attachment of alkyl chains to the PTI structure. Core level N 1s spectra can be divided into two components: 398.6 eV corresponding to C-N=C groups and 400.9 eV attributed to secondary and tertiary amines (NH/N-$(C)_3$) ((Figure S13 and S14).[19] An increase in the NH/N-$(C)_3$ peak was observed for the dodecyl-functionalised PTI compared to both FL-PTI and physisorption controls (Table S1). Quantitatively, the XPS data indicate 74 framework atoms per alkyl chain, comparing favourably with the TGA estimate of 101 atoms per chain. Controls of air quenched FL-PTI mixed with $C_{12}H_{25}Br$ and FL-PTI^{n-} with unreactive $C_{12}H_{26}$ showed similar TGA curves to the unfunctionalised FL-PTI, precluding a contribution from physisorption. The XPS measurements also exclude physisorption since the core level Br 3d was not observed in the grafted products, although it was visible in positive controls at relevant concentrations (Figure S15). Reaction with a shorter alkyl chain was also investigated; when charged FL-PTI reacted with octylbromide a mass loss of 12 wt% and the corresponding m/z peak at 57 were observed (Figure S16). XPS showed a similar increase in the NH/N-$(C)_3$ peak as observed for the dodecyl-functionalised PTI (Figure S17 and Table S1). In this case, XPS indicates one alkyl chain every 47 PTI atoms, closely matching the TGA estimate of one chain per 55 framework atoms. Given the uncertainties in these measurements, the agreement is excellent, and provides direct evidence of grafting to the PTI layers.

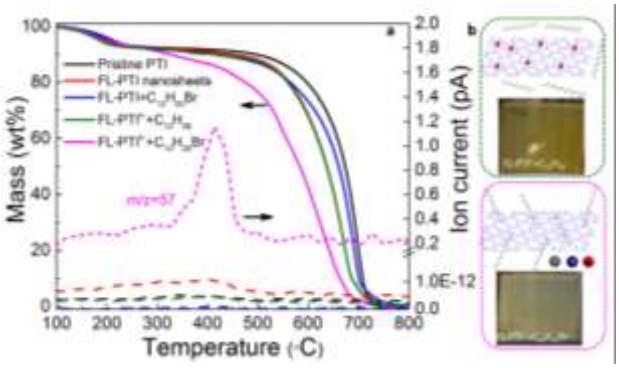

Figure 5. (a) TGA and TGA-MS (dashed) of pristine PTI and alkylated FL-PTI. Inset shows 100-400°C TGA region. (b) Photographs of control sample (top) and FL-PTI functionalised with dodecyl bromide (bottom).

The observed change in the XPS nitrogen components upon functionalization can be attributed to the attachment of alkyl chains to the nitrogen of the triazine ring. Density functional

theory (DFT) calculations suggest that the sodium ion bridges two triazine rings, with the extra electron delocalized over those two rings (Figure S19). The spin density associated with the extra electron has contributions on both C and N atoms of the rings; the high excess charge of 0.12|e| on the N atoms not directly interacting with Na, combined with their better accessibility compared to the C atoms of the PTI structure, suggest that the nitrogens are the most susceptible to react with the alkyl bromide molecule. Further study will be required to identify the specific mechanism. One possibility may be a single electron transfer, followed by free-radical addition, as hypothesised for other nanocarbons (Scheme S2).[20]

In summary, framework charging provides a new, simple route for exfoliation and functionalisation of PTI nanosheets, *via* NaNp/DMAc reduction. By avoiding damage, the intrinsic properties of the PTI structure can be retained and HR images indicate highly exfoliated hexagonal, crystalline FL-PTI nanosheets, averaging 1.1 nm thick (~3 layers) with AB stacking. The as-prepared FL-PTI solutions had a yield of 35 wt%, with excellent stability. Stabilized dispersions of FL-PTIs are useful feedstocks for a wide range of promising multifunctional applications. The relatively small flake size is particular relevant to potential applications in (electro)catalysis and photochemistry.[21] The FL-PTI^{n-} was successfully functionalised with alkyl chains *via* the framework charge, suggesting a route to a wide range of functionalised species to modulate surface chemistry and functional properties.

Acknowledgements

Financial support within framework of the European Flagship (grant agreement No. 696656–GrapheneCore1). CM acknowledges the award of a Royal Society University Research Fellowship by the UK Royal Society and the EPSRC award EP/K033840/1. Work by TS, TS, VB, FC, CAH and PFM at UCL was also supported by EPSRC grant EP/L017091/1.

Conflict of interest

The authors declare no conflict of interest.

References

[1] J. S. Zhang, Y. Chen, X. C. Wang, *Energ Environ Sci* **2015**, *8*, 3092-3108.
[2] M. Deifallah, P. F. McMillan, F. Cora, *J Phys Chem C* **2008**, *112*, 5447-5453.
[3] N. Mansor, T. S. Miller, I. Dedigama, A. B. Jorge, J. J. Jia, V. Brazdova, C. Mattevi, C. Gibbs, D. Hodgson, P. R. Shearing, C. A. Howard, F. Cora, M. Shaffer, D. J. L. Brett, P. F. McMillan, *Electrochim Acta* **2016**, *222*, 44-57.
[4] G. G. Zhang, Z. A. Lan, X. C. Wang, *Angew Chem Int Edit* **2016**, *55*, 15712-15727.
[5] a) P. Niu, L. L. Zhang, G. Liu, H. M. Cheng, *Adv Funct Mater* **2012**, *22*, 4763-4770; b) S. B. Yang, Y. J. Gong, J. S. Zhang, L. Zhan, L. L. Ma, Z. Y. Fang, R. Vajtai, X. C. Wang, P. M. Ajayan, *Adv Mater* **2013**, *25*, 2452-2456; c) T. Y. Ma, S. Dai, M. Jaroniec, S. Z. Qiao, *Angew Chem Int Edit* **2014**, *53*, 7281-7285; d) M. J. Bojdys, N. Severin, J. P. Rabe, A. I. Cooper, A. Thomas, M. Antonietti, *Macromol Rapid Comm* **2013**, *34*, 850-854; e) K. Schwinghammer, M. B. Mesch, V. Duppel, C. Ziegler, J. Senker, B. V. Lotsch, *J Am Chem Soc* **2014**, *136*, 1730-1733.
[6] a) E. Wirnhier, M. Doblinger, D. Gunzelmann, J. Senker, B. V. Lotsch, W. Schnick, *Chem-Eur J* **2011**, *17*, 3213-3221; b) S. Y. Chong, J. T. A. Jones, Y. Z. Khimyak, A. I. Cooper, A. Thomas, M. Antonietti, M. J. Bojdys, *J Mater Chem A* **2013**, *1*, 1102-1107.
[7] K. Schwinghammer, B. Tuffy, M. B. Mesch, E. Wirnhier, C. Martineau, F. Taulelle, W. Schnick, J. Senker, B. V. Lotsch, *Angew Chem Int Edit* **2013**, *52*, 2435-2439.
[8] T. S. Miller, T. M. Suter, A. M. Telford, L. Picco, O. D. Payton, F. Russell-Pavier, P. L. Cullen, A. Sella, M. S. P. Shaffer, J. Nelson, V. Tileli, P. F. McMillan, C. A. Howard, *Nano Lett* **2017**, *17*, 5891-5896.
[9] J. M. Englert, C. Dotzer, G. A. Yang, M. Schmid, C. Papp, J. M. Gottfried, H. P. Steinruck, E. Spiecker, F. Hauke, A. Hirsch, *Nat Chem* **2011**, *3*, 279-286.
[10] a) E. M. Milner, N. T. Skipper, C. A. Howard, M. S. P. Shaffer, D. J. Buckley, K. A. Rahnejat, P. L. Cullen, R. K. Heenan, P. Lindner, R. Schweins, *J Am Chem Soc* **2012**, *134*, 8302-8305; b) P. L. Cullen, K. M. Cox, M. K. Bin Subhan, L. Picco, O. D. Payton, D. J. Buckley, T. S. Miller, S. A. Hodge, N. T. Skipper, V. Tileli, C. A. Howard, *Nat Chem* **2017**, *9*, 244-249.
[11] A. J. Clancy, J. Melbourne, M. S. P. Shaffer, *J Mater Chem A* **2015**, *3*, 16708-16715.
[12] N. G. Connelly, W. E. Geiger, *Chem Rev* **1996**, *96*, 877-910.
[13] S. H. A. Axdal, D. D. L. Chung, *Carbon* **1987**, *25*, 377-389.
[14] a) S. Fogden, C. A. Howard, R. K. Heenan, N. T. Skipper, M. S. P. Shaffer, *Acs Nano* **2012**, *6*, 54-62; b) A. Penicaud, C. Drummond, *Accounts Chem Res* **2013**, *46*, 129-137.
[15] E. J. McDermott, E. Wirnhier, W. Schnick, K. S. Virdi, C. Scheu, Y. Kauffmann, W. D. Kaplan, E. Z. Kurmaev, A. Moewes, *J Phys Chem C* **2013**, *117*, 8806-8812.
[16] T. Morishita, A. J. Clancy, M. S. P. Shaffer, *J Mater Chem A* **2014**, *2*, 15022-15028.
[17] J. T. Yuan, J. J. Wu, W. J. Hardy, P. Loya, M. Lou, Y. C. Yang, S. Najmaei, M. L. Jiang, F. Qin, K. Keyshar, H. Ji, W. L. Gao, J. M. Bao, J. Kono, D. Natelson, P. M. Ajayan, J. Lou, *Adv Mater* **2015**, *27*, 5605-5609.
[18] H. Shin, J. W. Guan, M. Z. Zgierski, K. S. Kim, C. T. Kingston, B. Simard, *ACS Nano* **2015**, *9*, 12573-12582.
[19] D. Mitoraj, H. Kisch, *Angew Chem Int Edit* **2008**, *47*, 9975-9978.
[20] a) D. Voiry, O. Roubeau, A. Penicaud, *J Mater Chem* **2010**, *20*, 4385-4391; b) A. Clancy, M. Bayazit, S. Hodge, N. Skipper, C. Howard, M. Shaffer. *Chem. Rev.* 2018,. DOI:10.1021/acs.chemrev.8b00128.
[21] a) N. Mansor, J. J. Jia, T. S. Miller, T. Suter, A. B. Jorge, C. Gibbs, P. Shearing, P. F. McMillan, C. Mattevi, M. Shaffer, D. J. L. Brett, *ECS Transactions* **2016**, *75*, 885-897; b) W. R. Lee, Y. S. Jun, J. Park, G. D. Stucky, *J Mater Chem A* **2015**, *3*, 24232-24236.